Radius measurements of cataclysmic variable accretion disks

Paula Kvist

July 30, 2020

Contents

1 Cataclysmic variables

Cataclysmic variables (CVs) are interacting binary systems with a white dwarf primary and a low-mass secondary star. The secondary star fills its Roche lobe and transfers mass through the inner Lagrangian point of the system onto the white dwarf. Often the flowing gas forms an accretion disk around the white dwarf, where it circulates the primary and eventually falls down to the white dwarf surface. A hot spot (sometimes referred to as a bright spot) is created where the gas stream from the secondary hits the accretion disk.

Cataclysmic variables are divided into subgroups depending on their outburst behaviour, optical light curve and spectrum during the outburst. Classical novae have one recorded outburst. They typically brighten up to 6-19 magnitudes during their outburst. If a system has several recorded outbursts, it is classified as a recurrent nova. For both of these systems, the outbursts are explained by accretion of hydrogen-rich material onto the white dwarf surface, leading to an explosive thermonuclear runaway.

A different outburst mechanism is encountered in systems called dwarf novae. They go through recurrent outbursts with intervals ranging from dozens of days to years, experiencing fainter brightening than classical novae. Their outbursts are thought to originate from instabilities in accretion; a sudden increase in the mass transfer rate could release energy and increase the luminosity. Contrary to classical and recurrent novae, dwarf novae do not eject a shell of disk material in outburst.

The last subgroup, nova-like variables, show similar behaviour to other groups of cataclysmic variables in outburst, but have not erupted.

In this thesis, I will focus mostly on non-magnetic cataclysmic variables (especially dwarf novae) in quiescence. First, the standard model for the structure and components of cataclysmic variables is described, including modelling emission line formation from accretion disks. Afterwards a brief introduction to the dwarf nova OY Carinae will be provided and its accretion disk radius will be measured.

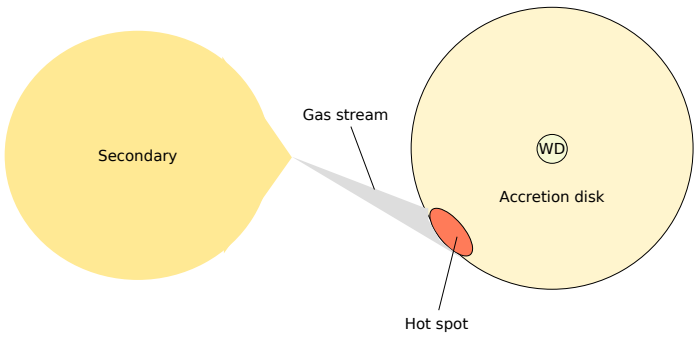

Figure 1: Simplistic stucture of a cataclysmic variable as seen face-on.

2 The standard model of cataclysmic variables

As the amount of observations increased on eclipsing cataclysmic variables, it became clear that they consist of several different components. Cataclysmic variables are binaries, with double-peaked emission line profiles (e.g. Balmer lines) indicating a prescence of a rotating disk. Later it was found that not all lines eclipse at the same time - and some might not eclipse at all! Including a wide range of ionization degrees, indicating a wide range of temperatures, it is now clear that cataclysmic variables host a variety of astrophysical phenomena originating from wildly different parts of the system.

The current standard model (Fig. 1) for cataclysmic variables consists on a white dwarf accompanied with a low-mass star. The companion star fills its Roche lobe, meaning it experiences mass overflow, which then accretes onto the white dwarf. This gas does not fall straight onto the white dwarf, but goes past it due to the angular momentum of the gas stream, and usually forms an accretion disk instead. The part where the gas stream hits the accretion disk is called the hot spot. In cataclysmic variables with strong magnetic fields, an accretion disk might not be formed. Instead, the gas stream accretes to the white dwarf following magnetic field lines.

2.1 Primary star

The primary object, the accreting star in the center of the accretion disk, is a white dwarf. White dwarfs are dense, electron-degenerate stellar remnants of low mass stars ($\lesssim 10M_{\odot}$). In cataclysmic variables, they are thought to be the remnants of binary component which was originally more massive, and thus evolved more quickly.

As the angular velocity of the accreting gas around the primary is a lot larger than that of the primary, a layer where the gas slows down before it hits the primary is formed. This layer is called the boundary layer. When the accreting media slows down, its kinetic energy transforms into radiation which irradiates the inner parts of the accretion disk. As the amount of radiation depends on the accretion rate, high accretion rates can lead to quite luminous boundary layers. (Warner 1995)

The average mass of white dwarfs in CVs is $\sim 0.84M_{\odot}$, which is larger than the average mass of single white dwarfs ($\sim 0.6M_{\odot}$). Zorotovic et al. (2011) provided two possible solutions to this problem: the white dwarf could gain mass by accretion or they could already have a greater mass while in post-common-envelope stage of the evolution of CVs. The first solution is rather uncomfortable, as it does not agree with current models of nova eruptions, in which the primary should lose more mass in outbursts than it accretes. The second solution might be a better match. It implies a stage of thermal time-scale mass transfer, when the primary could burn hydrogen in its surface in a stable manner and gain mass. However, this solution is not without its problems: it would predict a large population of cataclysmic variables with helium core primaries and evolved donor stars and those predictions do not match the observations (Wijnen, Zorotovic, and Schreiber 2015).

The flux from the accretion disk or the secondary is negligible compared to the flux of white dwarf in ultraviolet, which can be detected especially by Lyα absorption features in UV spectra. The temperatures of white dwarfs can be found by fitting model atmospheres to the UV spectra, as hotter white dwarfs have narrower Lyα profiles and steeper blue continua and cooler ones have broader line profiles and flatter continua. The temperatures range from about 12000K to tens of thousands of kelvins depending on how evolved the system is. Cataclysmic variables above the period gap[1] appear to have hotter primaries than those below it. (Pala et al. 2017)

[1]There is a deficiency of non-magnetic CVs with orbital periods of $2.3 \lesssim P_{orb}(\mathrm{h}) \lesssim 2.8$. This is referred to as a period gap.

2.2 Secondary star and its effect on the evolution of CVs

Secondaries in cataclysmic variables are Roche-lobe filling low-mass stars. Noting M_2 and R_2 as the mass and radius of the secondary and P_{orb} as the orbital period, a period-density relation

$$\langle \rho \rangle = \frac{M_2}{(4\pi/3)R_2^3} \simeq 107 P_{orb}^{-2}(\mathrm{h})\ \mathrm{g/cm}^3 \tag{1}$$

can be established for Roche-lobe filling secondaries (Warner 1995). In the earlier stages of cataclysmic variable evolution, the secondaries can be assumed to exhibit main sequence-like behaviour. The mass is somewhat proportional to the radius, although the secondaries in CVs are slightly oversized for their masses because they cannot quite maintain thermal equilibrium (Patterson et al. 2005, Knigge 2006). A relation between mass of the secondary and the orbital period of the system can be related by

$$\frac{M_2}{M_\odot} = 0.065 P_{orb}^{5/4}(\mathrm{h}). \tag{2}$$

Now it can be seen, that as the secondary loses mass to the primary, it should also shrink and the orbital period should shorten. In order of this to happen, angular momentum needs to be removed from the system. At this stage, it is removed by magnetic breaking in stellar winds of the secondary. This process goes on until the secondary has lost enough mass to become fully convective, losing the interface between radiative and convective regions which is thought to produce the magnetic field of the star (e.g. MacGregor and Charbonneau 1997). The angular momentum loss mechanism switches to gravitational radiation, which is not as efficient as magnetic breaking and does not support as great a mass loss rate. Radius of the star then shrinks below the Roche lobe and ceases the mass loss altogether. The loss of angular momentum still shrinks the orbit and with it the Roche lobe, and once it is small enough the mass transfer restarts. This detached phase is behind the period gap. (Knigge, Baraffe, and Patterson 2011)

After the system is below the period gap, the secondary continues to lose mass and the orbit of the system continues to shrink until the secondary is at the limit of being able to burn hydrogen. The mass-radius relation for substellar systems is inverse – the secondary responds to further mass loss by growing its radius. From Equation 1 it can be seen that as the density drops, the system begins to evolve towards longer periods again. Those systems are referred to as period-bouncers.

3 Accretion disks

As the secondary starts to lose mass, the gas stream it produces will miss the primary due to the angular momentum it has. In non-magnetic CVs the stream will initially form a thin ring around the white dwarf. The ring widens to a disk as some material loses energy and falls inwards, while a part of the initial ring will spread outwards to conserve angular momentum. (Warner 1995, and references therein) As the particles move in their orbits, they are destined to collide with each othes, causing them to heat up and then radiate the energy away. The particles lose energy and sink deeper towards the white dwarf. Thus, the gravitational potential is effectively transformed into radiation. (Pringle 1981; Frank, A. King, and Raine 2002)

Due to this relatively efficient release of radiation, the disk is the main source of emission in the visual wavelengths, producing a strong, blue continuum. In quiescence, the lines originating from the disk are double-peaked emission lines (as is shown in section 3.1). The most prominent feature is the emission lines of Balmer series of hydrogen at $\lambda\lambda 6563, 4861, 4340, 4101$ and 3970. Emission lines of neutral helium ($\lambda\lambda$6678, 5876, 5015, 4921, 4471, 4062) and singly ionized helium (λ4686) are often present. Other emission lines, for example singly ionized iron (λ5169) or doubly ionized nitrogen (λ4640) can be found as well, depending on the system (G. Williams 1983).

The emission is produced in parts of the disk where the optical thickness of the lines is much greater than that of the continuum. For Balmer lines, these conditions are met at the outer parts of the disk. Naturally the strength of the lines depends on system parameters; namely accretion rate, disk size and viscosity (R. E. Williams 1980). However, the mechanisms behind producing emission are unknown, as providing models that match the observations has proved to be difficult.

Viscosity plays a crucial form in accretion disk behaviour. The mechanism through which viscosity affects is still unknown, but for example magnetic fields and turbulent motions have been suggested as a driving force. Although the nature of the viscosity remains a mystery, some insights on how it affects the disk can be deduced: vertically it allows the angular momentum to be transferred outwards from inner areas, horizontally it heats up the gas and acts as a source of emission. (Smak 1984, Frank, A. King, and Raine 2002)

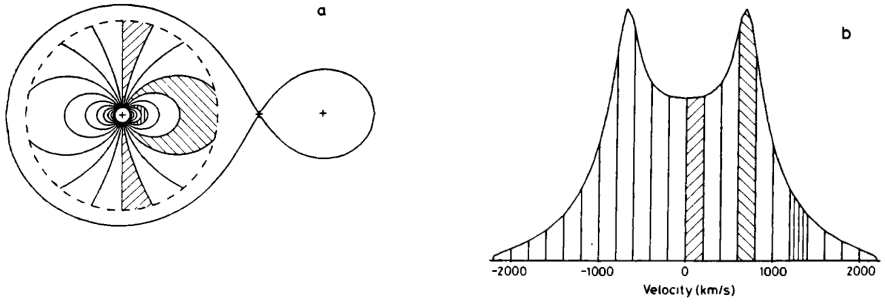

Figure 2: (a) Lines of constant radial velocity in a disk. (b) Corresponding velocity ranges in a line profile. From Horne and Marsh 1986.

3.1 Emission lines from accretion disks

The emission lines originating from accretion disks are characteristically double-peaked. They are broadened by Doppler shifts caused by the emitting disk materia orbiting the primary. Assuming that turbulent motions are small compared to disk width, the rotational velocity of the disk material can be approximated by Keplerian velocity:

$$v_K = \left(\frac{GM}{R}\right)^{1/2} \tag{3}$$

The Doppler velocity shift of this orbital motion depends on the inclination angle of the system i and azimuth angle relative to line-of-sight θ.

$$v_D = v_K \sin\theta \sin i \tag{4}$$

As can be seen in Figure 2a, the areas of constant velocities derived from Equation 4 form a dipole structure in the accretion disk. Each area of constant velocity corresponds to a different range in the emission line profile (Figure 2b). Areas near the inner radius form the emission seen in the line wings, emission from crescent-shaped areas that crop to the outer edge of the disk are seen in the peaks and the emission in the center of the line originates from the areas (almost) parallel to line-of-sight.

3.1.1 Emissivity function and construction of a line profile

The shape of the emission line depends on the distribution of emitting material. The general line shape can be constructed with the help of an emissivity function $f(r)$. In this approach, it is thought that the emissivity does not depend on the azimuthal angle, but only on radius. A popular form of the emissivity function is $f(r) \sim r^{-a}$, where the density of emitting atoms decreases with increasing radius to some power a (e.g. Smak 1981; Stover 1981).

Global line profile is constructed by summing all independent emission contributions within a range of r, weighted by the emissivity function $f(r)$. For a dimensionless inner radius r_1, outer radius of $r_2 = 1$ and corresponding dimensionless rotational velocities $v_1 = r_1^{-1/2}$ and $v_2 = 1$, Smak (1981) shows (corrected from Smak (1969)), that the profile can be described by integral

$$F(u) \sim \int_{r_0}^{r_z} \frac{r^{3/2} f(r) dr}{(1 - v_D^2 r)^{1/2}}, \tag{5}$$

where $r_z = \min(1, v_{D,max}^{-2})$. Equation 5 can be solved analytically for emissivity functions of the form $f(r) = r^{-a}$ with a an integer or half-integer, but must be solved numerically for other exponents.

The shape of the line Equation 5 provides is determined by parameters a, r_1 and $v_{D,max}$ (Figure 3.1.1). The value a determines the shape of the wings: larger values of a provide broader wings. Value of the inner radius, r_1, determines the velocity of the inner disk edge and thus the extent of the wings. Smaller values of r_1 means larger velocities and more extended wings. The velocity of the outer rim ($v_{D,max}$) determines the separation of the peaks.

Although this model is successful in describing the shape of emission lines in a simple enough way for optically thin media, an emissivity function independent of the azimuth angle does not work for optically thick disk. Shear broadening becomes important in modelling optically thick conditions. In small and moderate inclinations the effect of shear is negligible, but in large inclinations the central depression gains a V-shape, opposed to the U-shape seen in optically thin media. (Horne and Marsh 1986)

The inclination of the system affects the separation of the peaks as well. If the system has a low inclination and it's seen as almost edge-on, lines have only one peak. Material of the disk is not really moving towards or away from us, and broadening of the line by Doppler shifts is dominated by thermal broadening. Model lines for different inclinations are in Figure 3.1.1 for both optically thick and thin media.

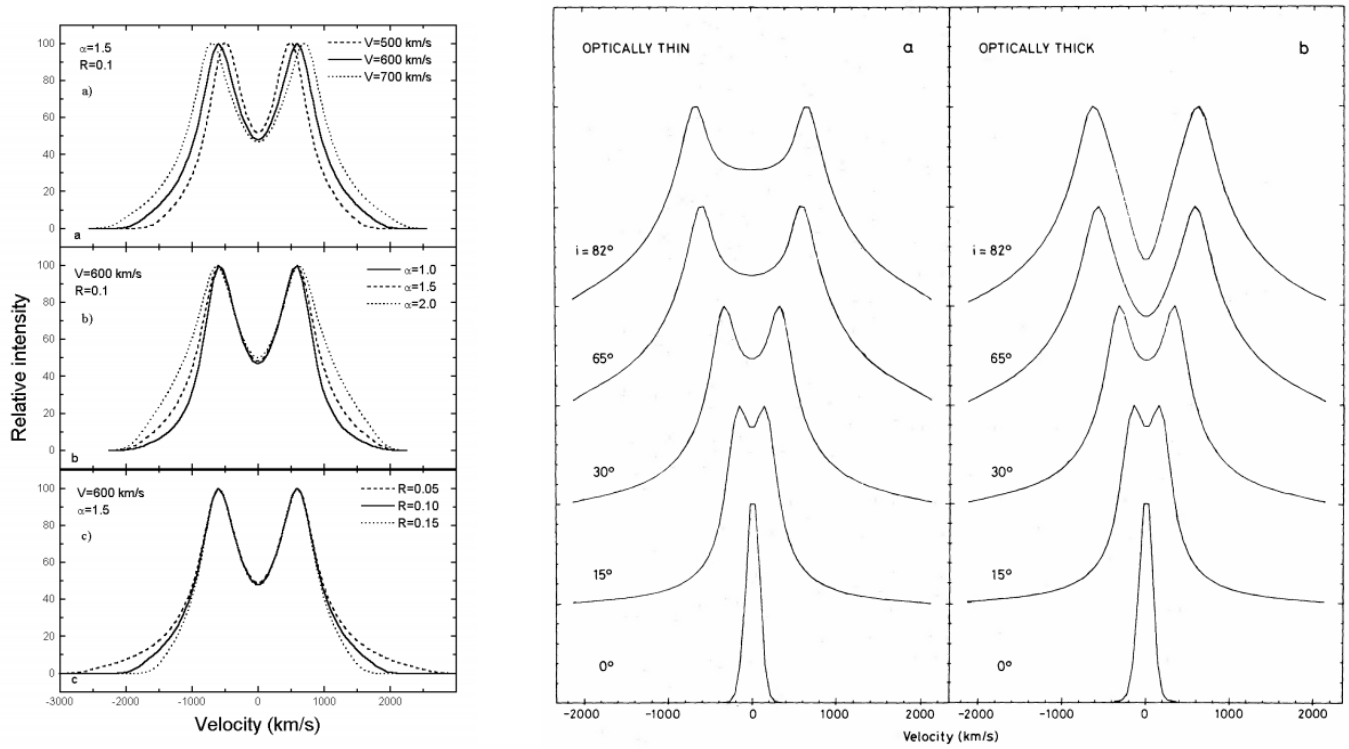

Figure 3: Left: How different parameter values affect the emission line profile. Rotational velocity of the outer rim (top) determines the peak separation. Exponent a of the emissivity function determine the broadness of the line. The inner disk radius defines the wing extension (Borisov and Neustroev 1997).

Figure 4: Right: Optically thin and thick double-peaked line profiles at different inclinations. The peaks become more defined at larger inclinations (Horne and Marsh 1986).

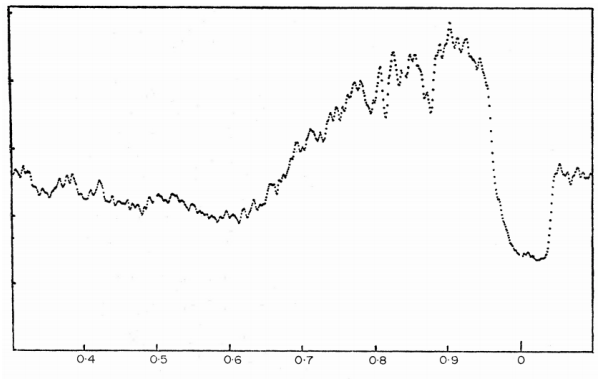

Figure 5: Orbital light curve of U Gem. The hot spot increases the luminosity remarkably for about half of the period. An eclipse of the primary can be seen at phase 0, after which the rotation of the hot spot behind the disk lowers the flux. The ingress of the hot spot can be seen as a hump (B. Warner and Nather 1971).

3.2 Hot spot

A hot spot is born when the gas stream hits the surface of the accretion disk (B. Warner and Nather 1971). The particles of the gas stream collides with those of the accretion disk, essentially transferring the kinetic energy of the stream into heat. As the gas of the disk then cools, it as well transmits radiation.

The hot spot is a variable source of emission, showing constant flickering with timescales of minutes. This flickering is seen in the light curves of all CVs, and it disappears during the hot spot eclipse. In eclipsing systems, where hot spot luminosity is comparable to accretion disk luminosity, the presence of the hot spot can be seen as a hump in the light curve, lasting to about half of the period. The disappearance is caused by optically thick disk; when hot spot is eclipsed by the disk, it does not contribute to observed light.

The effects of the hot spot on the light curve of a CV is well demonstrated in U Gem (Figure 5). It is a dwarf nova system with the hot spot contributing to a significant part of the total luminosity. The hot spot is behind the disk at phases $\sim 0.1 - 0.6$. The hump at phases $\sim 0.6 - 0.9$ is caused by light emitting from the hot spot; it's flickering can also be seen clearly. An eclipse of the hot spot can be seen at phase ~ 0, where the flickering also ceases.

The hot spot is the cause for an observed "S-wave" as well (Fig. 6). It is a source of mainly hydrogen and helium emission (but can contribute to other lines as well), and contributes to the observed lines together with the emission from the disk. As the hot spot turns towards us, the emission from it is blueshifted and thus strengthens the blue peaks; as it retreats, it strengthens the red peaks as the emission is redshifted. If a trailed spectrum is taken, this is seen as the line "swaying" from blue to red, forming an s-shape.

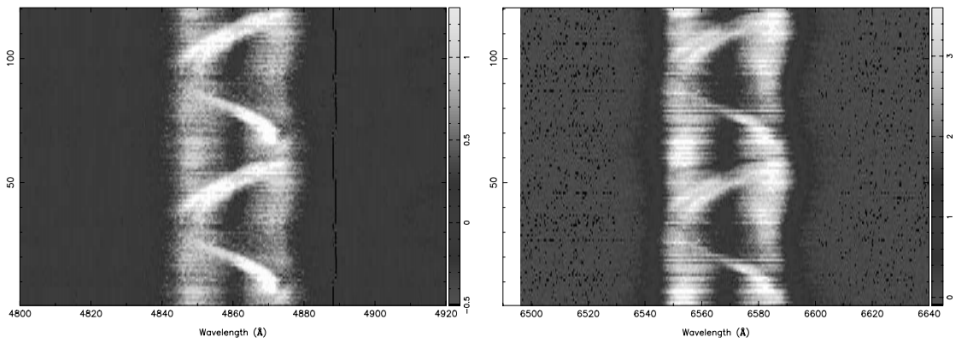

Figure 6: Trailed spectrum of WZ Sge showing S-waves of Hβ (left) and Hα (right) originating from the hot spot (Skidmore et al. 2000).

3.3 Size and shape of the accretion disk

At a large enough distance from the white dwarf, the gravitational influence of the secondary distorts the gas stream orbits, causing them to overlap instead of following Keplerian trajectories. This causes dissipation, which prevents the disk from growing any larger. This tidal truncation radius can be approximated by (Paczynski 1977, Warner 1995)

$$\frac{r_{d,max}}{a} = \frac{0.6}{1+q}, \qquad 0.03 < q < 1. \tag{6}$$

The disk is not strictly speaking circular, but slightly elongated perpendicular to the line connecting the stars (Figure 7). In systems with low-mass secondaries, the disk becomes tidally unstable and settles to an eccentric, periodically oscillating state instead of a disk rotating in the frame of the binary. The oscillation period is slightly longer than the binary period, and it can be seen as characteristic superhumps in the light curves of SU UMa type stars in superoutbursts (Whitehurst 1988). The tidal instability of the accretion disk causing this behaviour grows when the disk extends beyond 3:1 resonance radius. (Hirose and Osaki 1990).

There are several methods that have been used to measure the disk radius. The keplerian velocity of the outer rim can be measured from emission line peak separation of H_α line. Forming H_α line requires lower excitation energies than other Balmer lines, and it can be used to trace cooler gas of the outer disk. The radius can then be calculated from Equation 3, if the mass of the primary is known. This method of radius measurement is later demonstrated in the case of OY Carinae.

The precision of this method is mostly affected by the spectral resolution of the spectrograph used for observations (and of course, the precision of mass measurements, inclination and other parameters used in calculations). However,

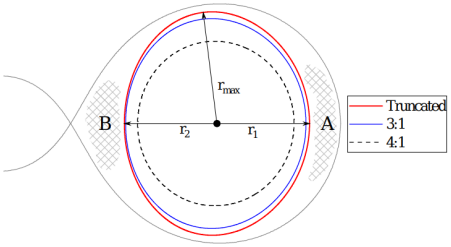

Figure 7: Tidal truncation limit (red), 3:1 (blue) and 4:1 (black, dashed) resonance orbits for a restricted three-body problem with mass ratio $q = 0.15$ (Neustroev and Zharikov 2019).

the emission line peaks are usually distinct even with quite bad spectral resolution, making measurements reliable. The peak-to-peak separation should vary throughout the orbital period because of the disk elongation, but the effects can be cancelled by measuring on orbit-averaged spectra.

Other methods of radius measurement rely on analysing eclipse light curves. In eclipse mapping method (developed by Horne (1985)) model light curves are produced, and the system parameters are adjusted until the model light curves match observed ones. This method has been demonstrated by e.g. Zhang et al. (1986) and Feline et al. (2005) in measuring the system parameters for several CVs. The accretion disk radius derived for HT Cas in quiescence by both of them ($\sim 0.22 - 0.24a$) is smaller than that derived later by Neustroev et al. (2016) ($\sim 0.52a$), who measured the radius from H_α emission line. However, it could be a result from assuming the hot spot to lie at the outer rim of the disk, which it does not necessarily do; Skidmore et al. (Skidmore et al. 2000) found the accretion stream to infiltrate to the disk, allowing the hot spot to lie more inwards.

The disk instability model used for modelling outburst behaviour in novae predicts that the disk size should vary, depending on if the system is in quiescence or outburst. According to this model, the radius should increase close to the tidal truncation limit during outburst, and shrink while in quiescence (Smak 1971, Lasota 2001) The radii of disks obtained from the eclipse mapping method agree well with this model. However, Neustroev et al. (2016) found that when measured from the peak-to-peak distance of H_α emission line, the radius of HT Cas was consistently large and close to the tidal truncation limit. It is later shown that using this method, the radius of OY Carinae in quiescence is large and close to the tidal truncation limit as well.

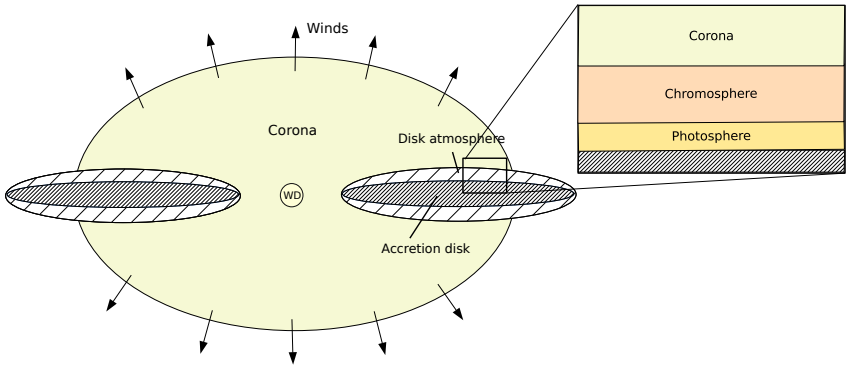

Figure 8: Schematic picture of the structure of the primary and accretion disk.

3.4 Vertical structure of the accretion disk

It is possible to discuss the vertical and horizontal structure of accretion disks separately. Several models exists for the vertical structure, practically all of them starting with the equations of hydrostatic equilibrium, energy transport, flux generation and mass conservation (e.g. Meyer and Meyer-Hofmeister 1982, Cannizzo and Wheeler 1984). A vertical structure can lead to thermal instabilities, and thus explain some of the outburst behaviour seen in cataclysmic variables (e.g. Smak 1982) and the formation of a corona above the disk (Shaviv and Wehrse 1986).

Even before the modelling of vertical structure, some differences in observed colours of inclined disks were found, and suggestions arose of emission areas outside the photosphere of the disk (Schwarzenberg-Czerny 1981, and references therein). Radiation emerging from the central areas (i.e., boundary layer, surface of the primary, or hot, inner parts of the disk) could be strong enough to ionize the upper layers of the disk, forming a cromosphere above the photosphere. The chromosphere could account to UV line intensities of Lα, He II λ 1640, N V, C IV and Si IV. They are states of higher ionization and could not form in the optically thin parts of the disk (Jameson, A. R. King, and Sherrington 1980).

The irradiation of the primary or the boundary layer also causes material from the inner disk to evaporate into a hot corona. This corona in turn flows heat downwards to the cromosphere. Some of the coronal material is eventually accreted into the white dwarf, while some may escape as winds. The winds from the accretion disk can strengthen substantially (and are mainly observed) during outbursts, when the increased radiation can dissipate the whole coronal layer. (Meyer and Meyer-Hofmeister 1994)

Cataclysmic variables show evidence of winds especially in UV wavelengths (e.g. C IV, N V, Si IV) and He II λ4686 line. These lines can show similar eclipse behaviour (but do not necessarily) as lines originating from the disk, but are single-peaked. In addition, these spectral lines are blueshifted with linewidths indicating terminal velocities comparable to escape velocities. These winds have been observed for example in UX UMa (Holm, Panek, and Schiffer 1982) and TW Vir (Cordova and Mason 1982). In dwarf novae, winds are observed only in outburst; in quiescence, lines mentioned before disappear.

4 OY Carinae

OY Carinae (hereafter shortened to OY Car) is a well-known and well-studied system in the world of cataclysmic variables. It is a SU UMa-type dwarf nova with orbital period of ~ 91 minutes. The short period coupled with high inclination makes OY Car a fruitful object, and many photometric studies have been done to determine it's parameters. For this thesis, system parameters derived by Littlefair et al. (2008) are used:

- inclination $i = 83.3^o \pm 0.2^o$
- primary mass $M_1 = (0.84 \pm 0.04)M_\odot$
- separation $a = (0.65 \pm 0.01)R_\odot$.
- mass ratio $q = 0.102 \pm 0.003$

4.1 Observations on X-SHOOTER

The datasets were taken by Copperwheat et al. (2012) on VLT X-SHOOTER. The observations were done on two nights: 4.2.2009 and 10.2.2009. All three arms (UVB, VIS, NIR) were used with slit widths of 1.0, 1.2 and 0.9, respectively, with spectral resolutions of 0.7Å, 1Å and 2.9Å. Both datasets consist on 28 spectra for each arm with exposure times of 185, 180 and 205 seconds. The reductions of the data were done with data reduction tool Gasgano (provided by ESO) using X-SHOOTER pipelines. The resulting combined spectra of the observations on 10.2.2009 are in Figure 9, with main spectral features identified.

Telluric features riddle some areas especially in UVB and NIR (where wavelengths $>$ 1370 nm are cut off), but most of the lines are uninterrupted. The emission lines are double-peaked. The Balmer series of hydrogen can be clearly seen on the optical wavelengths, as well as some strong HeI lines. Shallow absorption dips from the primary can be seen on the edges of Balmer lines. In NIR, emission lines of calsium are found, and in the shorter wavelengths of UVB range, an "iron curtain" of iron lines can be distinguished as absorption features.

4.2 Radius of the accretion disk

The radius measurements were done from measuring the H_α emission line peaks as described in section 3.3 The orbital velocities were calculated from the peak wavelengths λ_r and λ_l (for right and left peak, respectively), central wavelength λ_c and inclination i:

$$v_K = \frac{\lambda_r - \lambda_l}{\lambda_c} c \sin i. \tag{7}$$

The outer radius of the emitting area was then calculated from Equation 3. The measurements were done for all Balmer lines, and the rotational velocity

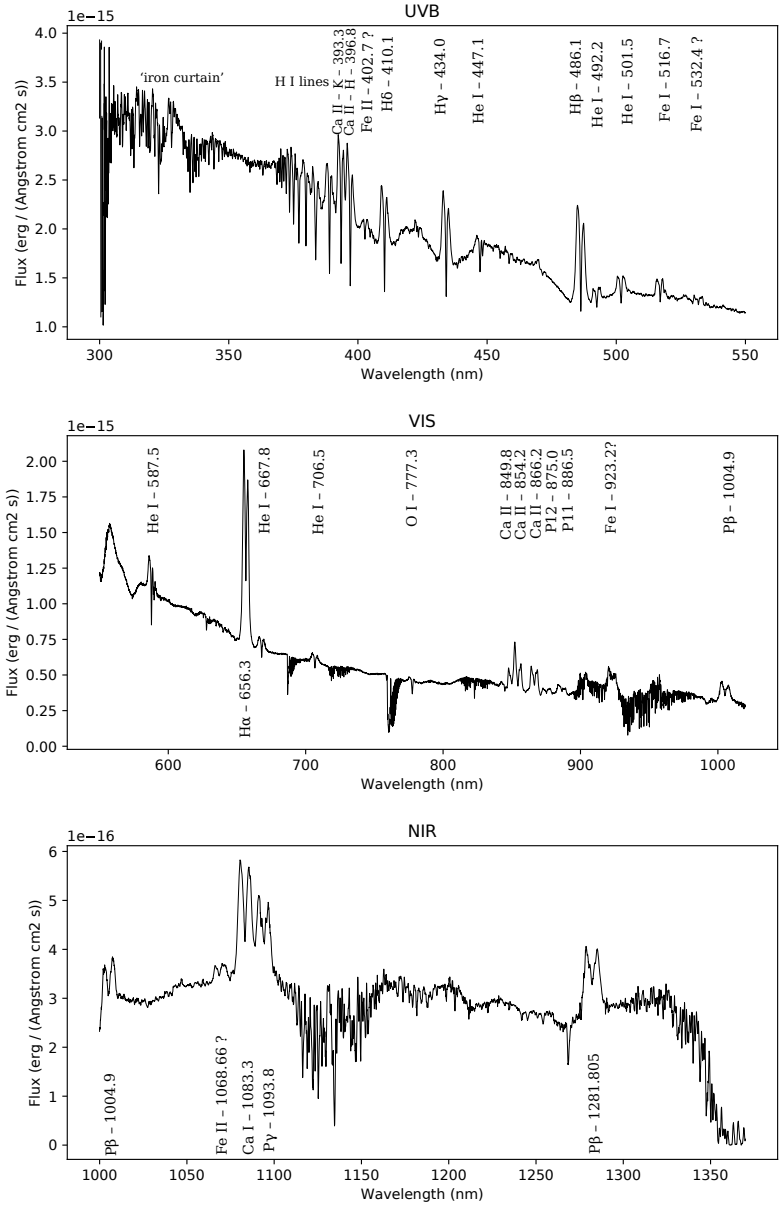

Figure 9: Combined spectra taken on 10.2.2009 with X-Shooter. Most prominent features in UVB arm (top panel) show a forest of iron lines, HI lines and lines of Balmer series. VIS arm (middle panel) shows H_α and lines of helium and calsium. NIR arm (bottom panel) shows some lines of phosphorus, iron and calsium. Most of the NIR arm was riddled with atmospheric interruption and showed no lines, so it was cropped off.

and radius from each line can be seen in Table 1. The largest uncertainty in velocities is caused by the spectral resolution; for VIS arm, where H_α is found, this corresponds to velocity uncertainty of $\pm$45km/s and radius uncertaintly of $\pm 0.04a$.

	spectral line	v_K (km/s)	radius (a)
4.2.	H_α	664	0.56
	H_β	761	0.43
	H_γ	903	0.30
	H_δ	849	0.34
10.2.	H_α	649	0.59
	H_β	730	0.46
	H_γ	676	0.54
	H_δ	673	0.55

Table 1: Rotational velocities and radii of areas emitting Balmer lines.

The tidal truncation radius for OY Car calculated from equation 6 is $0.54a$. The measured radius of the disk is slightly larger than the tidal truncation radius, but within the margin of error. This result contradicts previous models of the radius evolution and previous radius measurements for OY Car. For example, Wood et al. (1989) measured the radius of the disk to be $R_D = 0.313a$ from the hot spot eclipses. However, this contradiction could between measurements from eclipse mapping method and peak-to-peak separation could be avoided by assuming, that the hot spot does not lie at the disk edge, but closer to the white dwarf.

5 Summary

The main picture of the structure of cataclysmic variables is already well-established, although discussion about the details is still greatly needed. The radius of the accretion disk is a part of this discussion. The radius of the accretion disk has been thought to evolve as a result of the outburst cycle since the 80's. However, recently there has been evidence of the radius staying about a constant through both outburst and quiescence, contradicting previous theories and observations (Neustroev, Zharikov, and Borisov 2016).

This contradiction could be caused simply by different methods in measurements. Eclipse mapping has been a popular method due to its reasonably good precision and capability of resolving numerous system parameters from the same observations (Horne 1985, Feline et al. 2005). However, in radii measurements, it assumes the hot spot to lie at the outer rim of the disk. It has now been found out, that it might locate closer to the white dwarf (Skidmore et al. 2000).

Measuring the radius from peak-to-peak separation of H_α line does not make this assumption, and thus provides larger radii close or over the tidal truncation radius. The radius of OY Carinae was measured using this method to be $(0.56 - -0.59)a \pm 0.04a$, while the tidal truncation radius is $0.54a$. This supports the results of Neustroev et al. (2016).

References

Borisov, N. V. and V. V. Neustroev (Jan. 1997). "Modelling emission line profiles of a non-uniform accretion disk". In: *Bulletin of the Special Astrophysics Observatory* 44, pp. 110–118. arXiv: astro-ph/9806159 [astro-ph].

Cannizzo, J. K. and J. C. Wheeler (July 1984). "The vertical structure and stability of alpha model accretion disks." In: *Astrophysical Journal, Suppl. Ser.* 55, pp. 367–388. DOI: 10.1086/190959.

Copperwheat, C. M. et al. (Mar. 2012). "A J-band detection of the donor star in the dwarf nova OY Carinae and an optical detection of its 'iron curtain'". In: *Monthly Notices of the Royal Astronomical Society* 421.1, pp. 149–158. DOI: 10.1111/j.1365-2966.2011.20282.x. arXiv: 1111.6775 [astro-ph.SR].

Cordova, F. A. and K. O. Mason (Sept. 1982). "High-velocity winds from a dwarf nova during outburst." In: *Astrophysical Journal* 260, pp. 716–721. DOI: 10.1086/160291.

Feline, W. J. et al. (Dec. 2005). "ULTRACAM photometry of the eclipsing cataclysmic variables GY Cnc, IR Com and HT Cas". In: *Monthly Notices of the Royal Astronomical Society* 364.4, pp. 1158–1167. DOI: 10.1111/j.1365-2966.2005.09668.x. arXiv: astro-ph/0510438 [astro-ph].

Frank, Juhan, Andrew King, and Derek J. Raine (2002). *Accretion Power in Astrophysics: Third Edition.*

Hirose, Masahito and Yoji Osaki (Feb. 1990). "Hydrodynamic Simulations of Accretion Disks in Cataclysmic Variables: Superhump Phenomenon in SU UMa Stars". In: *Publications of the Astronomical Society of Japan* 42, pp. 135–163.

Holm, A. V., R. J. Panek, and III Schiffer F. H. (Jan. 1982). "Ultraviolet spectrum variability of UX UMa." In: *Astrophysical Journal* 252, pp. L35–L37. DOI: 10.1086/183714.

Horne, K. (Mar. 1985). "Images of accretion discs I. The eclipse mapping method." In: *Monthly Notices of the Royal Astronomical Society* 213, pp. 129–141. DOI: 10.1093/mnras/213.2.129.

Horne, K. and T. R. Marsh (Feb. 1986). "Emission line formation in accretion discs". In: *Monthly Notices of the Royal Astronomical Society* 218, pp. 761–773. DOI: 10.1093/mnras/218.4.761.

Jameson, R. F., A. R. King, and M. R. Sherrington (May 1980). "The UV spectrum of AE Aqr." In: *Monthly Notices of the Royal Astronomical Society* 191, pp. 559–569. DOI: 10.1093/mnras/191.3.559.

Knigge, Christian (Dec. 2006). "The donor stars of cataclysmic variables". In: *Monthly Notices of the Royal Astronomical Society* 373.2, pp. 484–502. DOI: 10.1111/j.1365-2966.2006.11096.x. arXiv: astro-ph/0609671 [astro-ph].

Knigge, Christian, Isabelle Baraffe, and Joseph Patterson (June 2011). "The Evolution of Cataclysmic Variables as Revealed by Their Donor Stars". In: *The Astrophysical Journal Supplement* 194.2, 28, p. 28. DOI: 10.1088/0067-0049/194/2/28. arXiv: 1102.2440 [astro-ph.SR].

Lasota, Jean-Pierre (June 2001). "The disc instability model of dwarf novae and low-mass X-ray binary transients". In: *New Astronomy Reviews* 45.7, pp. 449–508. DOI: 10.1016/S1387-6473(01)00112-9. arXiv: astro-ph/0102072 [astro-ph].

Littlefair, S. P. et al. (Aug. 2008). "On the evolutionary status of short-period cataclysmic variables". In: *Monthly Notices of the Royal Astronomical Society* 388.4, pp. 1582–1594. DOI: 10.1111/j.1365-2966.2008.13539.x. arXiv: 0806.1129 [astro-ph].

MacGregor, K. B. and P. Charbonneau (Sept. 1997). "Solar Interface Dynamos. I. Linear, Kinematic Models in Cartesian Geometry". In: *The Astrophysical Journal* 486.1, pp. 484–501. DOI: 10.1086/304484.

Meyer, F. and E. Meyer-Hofmeister (Feb. 1982). "Vertical structure of accretion disks". In: *Astronomy & Astrophysics* 106.1, pp. 34–42.

— (Aug. 1994). "Accretion disk evaporation by a coronal siphon flow." In: *Astronomy & Astrophysics* 288, pp. 175–182.

Neustroev, V. V. and S. V. Zharikov (Aug. 2019). "Voracious vortexes in cataclysmic variables: II. Evidence for the expansion of accretion disc material beyond the accretor's Roche-lobe". In: *arXiv e-prints*, arXiv:1908.10867, arXiv:1908.10867. arXiv: 1908.10867 [astro-ph.SR].

Neustroev, V. V., S. V. Zharikov, and N. V. Borisov (Feb. 2016). "Voracious vortexes in cataclysmic variables. A multi-epoch tomographic study of HT Cassiopeia". In: *Astronomy & Astrophysics* 586, A10, A10. DOI: 10.1051/0004-6361/201526363. arXiv: 1506.04753 [astro-ph.SR].

Paczynski, B. (Sept. 1977). "A model of accretion disks in close binaries." In: *The Astrophysical Journal* 216, pp. 822–826. DOI: 10.1086/155526.

Pala, A. F. et al. (Apr. 2017). "Effective temperatures of cataclysmic-variable white dwarfs as a probe of their evolution". In: *Monthly Notices of the Royal Astronomical Society* 466.3, pp. 2855–2878. DOI: 10.1093/mnras/stw3293. arXiv: 1701.02738 [astro-ph.SR].

Patterson, Joseph et al. (Nov. 2005). "Superhumps in Cataclysmic Binaries. XXV. q_{crit}, $\in(q)$, and Mass-Radius". In: *The Publications of the Astronomical Society of the Pacific* 117.837, pp. 1204–1222. DOI: 10.1086/447771. arXiv: astro-ph/0507371 [astro-ph].

Pringle, J. E. (Jan. 1981). "Accretion discs in astrophysics". In: *Annual review of astronomy and astrophysics* 19, pp. 137–162. DOI: 10.1146/annurev.aa.19.090181.001033.

Schwarzenberg-Czerny, A. (Jan. 1981). "Radiation from the discs in cataclysmic variables : the chromosphere." In: *Acta Atronomica* 31, pp. 241–265.

Shaviv, G. and R. Wehrse (Apr. 1986). "The vertical temperature stratification and corona formation of accretion disc atmospheres". In: *Astronomy & Astrophysics* 159.1-2, pp. L5–L7.

Skidmore, Warren et al. (Oct. 2000). "Investigating the structure of the accretion disc in WZ Sge from multiwaveband time-resolved spectroscopic observations - I". In: 318.2, pp. 429–439. DOI: 10.1046/j.1365-8711.2000.03781.x.

Smak, J. (Jan. 1969). "On the Rotational Velocities of Gaseous Rings in Close Binary Systems". In: *Acta Astronomica* 19, p. 155.

Smak, J. (Jan. 1971). "Eruptive Binaries. II. U Geminorum". In: *Acta Astronomica* 21, p. 15.

— (Jan. 1981). "On the emission lines from rotating gaseous disks." In: *Acta Astronomica* 31, pp. 395–408.

— (Jan. 1982). "Accretion in cataclysmic binaries. I - Modified alpha-disks with convection". In: *Acta Astronomica* 32.3-4, pp. 199–211.

— (Jan. 1984). "Outbursts of dwarf novae." In: *Publications of the Astronomical Society of the Pacific* 96, pp. 5–18. DOI: 10.1086/131295.

Stover, R. J. (Sept. 1981). "Time-resolved spectroscopy of cataclysmic variables : U Gem." In: *The Astrophysical Journal* 248, pp. 684–695. DOI: 10.1086/159193.

Warner (Jan. 1995). "Cataclysmic variable stars". In: *Cambridge Astrophysics Series* 28.

Warner, B. and R. E. Nather (Jan. 1971). "Observations of rapid blue variables - II. U Geminorum." In: *Monthly Notices of the Royal Astronomical Society* 152, p. 219. DOI: 10.1093/mnras/152.2.219.

Whitehurst, Robert (May 1988). "Numerical simulations of accretion discs - I. Superhumps : a tidal phenomenon of accretion discs." In: *Monthly Notices of the Royal Astronomical Society* 232, pp. 35–51. DOI: 10.1093/mnras/232.1.35.

Wijnen, T. P. G., M. Zorotovic, and M. R. Schreiber (May 2015). "White dwarf masses in cataclysmic variables". In: *Astronomy & Astrophysics* 577, A143, A143. DOI: 10.1051/0004-6361/201323018. arXiv: 1503.05197 [astro-ph.SR].

Williams, G. (Nov. 1983). "Spectroscopy of cataclysmic variables. I. Observations." In: *The Astrophysical Journal Supplement Series* 53, pp. 523–552. DOI: 10.1086/190900.

Williams, R. E. (Feb. 1980). "Emission lines from the accretion disks of cataclysmic variables." In: *Astrophysical Journal* 235, pp. 939–944. DOI: 10.1086/157698.

Wood, Janet H. et al. (June 1989). "Eclipse Studies of the Dwarf Nova OY Carinae in Quiescence". In: *The Astrophysical Journal* 341, p. 974. DOI: 10.1086/167557.

Zhang, E. -H., E. L. Robinson, and R. E. Nather (June 1986). "The Eclipses of Cataclysmic Variables. I. HT Cassiopeiae". In: *The Astrophysical Journal* 305, p. 740. DOI: 10.1086/164288.

Zorotovic, M., M. R. Schreiber, and B. T. Gänsicke (Dec. 2011). "Post common envelope binaries from SDSS. XI. The white dwarf mass distributions of CVs and pre-CVs". In: *Astronomy & Astrophysics* 536, A42, A42. DOI: 10.1051/0004-6361/201116626. arXiv: 1108.4600 [astro-ph.SR].